TECHNICAL MEMORANDUM

410

A cloud scheme for data assimilation purposes: Description and initial tests

A. M. Tompkins and M. Janisková

Research Department

Submitted to Q. J. Roy. Meteor. Soc.

July 2003

This paper has not been published and should be regarded as an Internal Report from ECMWF. Permission to quote from it should be obtained from the ECMWF.

European Centre for Medium-Range Weather Forecasts
Europäisches Zentrum für mittelfristige Wettervorhersage
Centre européen pour les prévisions météorologiques à moyen terme

For additional copies please contact

The Library
ECMWF
Shinfield Park
Reading
RG2 9AX
library@ecmwf.int

Series: ECMWF Technical Memoranda

A full list of ECMWF Publications can be found on our web site under:
http://www.ecmwf.int/publications/

©Copyright 2003

European Centre for Medium Range Weather Forecasts
Shinfield Park, Reading, RG2 9AX, England

Literary and scientific copyrights belong to ECMWF and are reserved in all countries. This publication is not to be reprinted or translated in whole or in part without the written permission of the Director. Appropriate non-commercial use will normally be granted under the condition that reference is made to ECMWF.

The information within this publication is given in good faith and considered to be true, but ECMWF accepts no liability for error, omission and for loss or damage arising from its use.

Abstract

A new cloud scheme has been developed specifically for the purposes of variational data assimilation; a task complicated by the inherent nonlinearity of many cloud processes. The aim was to retain the central aspects of the scheme used in the nonlinear forecast model, while removing much of the complexity and as many of the discrete transitions as possible. The scheme thus retains a simplified link to convective detrainment, and uses a similar formulation for the production of precipitation. A flexible statistical cloud scheme approach is used, where the diagnosis of stratiform cloud fraction and condensate amount depend on assumptions concerning subgrid-scale fluctuations. A novel aspect of the new scheme is the treatment of precipitation evaporation that specifically takes this subgrid distribution of humidity variability into account.

The scheme is tested by comparing physical tendencies of thermodynamical quantities, calculated for a series of input temperature and humidity profiles, to those produced by the complex prognostic cloud scheme used in the forecast model. This is conducted over three sites in North America and the Tropical Western Pacific, and the new diagnostic scheme is found to give comparable results to the full forecast model for radiation and cloud observations. As a further test, a series of model integrations are performed, with the full prognostic scheme used in operational forecasts replaced in turn by the nonlinear versions of the current operational assimilation diagnostic cloud scheme, and then by the new scheme described here. Using the prognostic scheme as a metric, the new scheme improves on the current assimilation cloud scheme for many attributes such as cloud cover and ice water content, both in the tropics and mid-latitudes. In particular the new diagnostic scheme addresses the overriding weakness of the current diagnostic scheme which produces almost no precipitation in the tropics.

Tangent linear and adjoint versions of the new scheme have been constructed and it is demonstrated that the scheme can successfully and robustly perform tangent linear integrations for a 12 hour window, and significantly improves the tangent linear approximation of the simplified linearized model to finite difference calculations using the full nonlinear forecast model.

1 Introduction

Data assimilation forms a crucial component of any forecast system, aiming to provide the forecast model with the most accurate possible initial state, to which forecast errors are critically sensitive (Courtier et al., 1994, Rabier et al., 1996). A number of forecast centres have successfully introduced or are in the process of implementing a four dimensional variational analysis (4D-Var) approach which determines the trajectory that minimises the differences to the observations and the model background state over a specific time window (Rabier et al., 1998).

In order to perform the minimization in variational data assimilation efficiently, the tangent-linear models and their adjoints are required. The incremental formulation of 4D-Var (Courtier et al., 1994), which is used at ECMWF, allows the minimization to be performed with a simplified linear model (using an adiabatic model and lower resolution). The quality of the tangent-linear approximation affects the performance of the analysis system (Rabier et al., 1998), and as discussed in several studies (Janisková et al., 1999, Mahfouf, 1999, Mahfouf and Rabier, 2000), this can be gradually improved by introducing physical processes. The first set of linearized physics used in the ECMWF 4D-Var system (Mahfouf, 1999) will be upgraded by including a more sophisticated radiation scheme. However, the radiation scheme will still be combined with the simple diagnostic cloud scheme described by Janisková et al. (2002b), which has a number of weaknesses, not least the lack of large-scale precipitation production in the tropics. For further improvement of the forecast system, and also to enable the future assimilation of cloud and precipitation data, a more comprehensive description of the moist processes of convection and cloud is essential (Janisková et al., 2002a).

One factor inhibiting cloud scheme evolution is the inherent nonlinearity of latent heat release and associated precipitation formation; and here lies the crux of the assimilation dilemma. It is desirable to have a linearized

model that approximates as closely as possible the sensitivity of the full nonlinear model. If this is not so, the forecast model may not be in balance with its own analysis, resulting in problems of model spin-up. Additionally, multi-incremental approaches that separate successive minimizations of the linear system with nonlinear full integrations can suffer from discrete transitions, affecting the stability of the overall minimization process (Mahfouf and Rabier, 2000). However, the nonlinear models have steadily evolved in complexity in order to improve forecast skill, usually involving the inclusion of highly nonlinear processes that are often controlled by threshold 'switches'. For example, the prognostic cloud scheme introduced into the ECMWF according to Tiedtke (1993) and Jakob (2002) includes a plethora of such thresholds. Even if it were possible to construct the tangent linear and adjoint versions of this complex scheme, the range of their validity would be restricted due to these thresholds, and their value would be questionable. Indeed,Janisková et al. (1999), Mahfouf (1999) and Laroche et al. (2002) found that without the implementation of specific methods to remove nonlinearities in the diffusion schemes for instance, it was not possible to achieve a functional assimilation system at all.

A compromise has to be found, with a 'smooth' tangent linear model containing as few discrete 'on/off' processes as possible, while still honouring the most important aspects of the full nonlinear scheme. The aim of this paper is to outline such a scheme to represent stratiform cloud processes in the ECMWF 4D-Var system. In order to avoid discreteness, it was necessary to retain a suitable level of simplicity throughout, which is also constrained by the numerical efficiency requirements of any forecast system. The scheme that is developed is therefore less complex than the stratiform cloud scheme recently described by Lopez (2002), which included prognostic equations for cloud and precipitation amounts. A prognostic formulation of precipitation necessitates the complexity of a semi-Lagrangian advection scheme or much shorter timesteps. A diagnostic form is already used in the full Tiedtke (1993) scheme, and Ghan and Easter (1992) demonstrated that such an approach is not necessarily detrimental. A prognostic cloud water relationship is left to future development, which could possibly incorporate a total water control variable.

The paper is outlined as follows: The following section briefly recalls the existing operational 4D-Var diagnostic cloud scheme, which shall be referred to as *OPERDIAG*, highlighting some of the weaknesses of the present approach, while section 3 introduces the new diagnostic cloud scheme (*NEWDIAG*). Section 4 compares these two diagnostic schemes and the operational prognostic scheme of Tiedtke (1993) (*OPERPROG*) to cloud and radiation observations from the Atmospheric Radiation Measurement (ARM) program sites. Section 5 then describes forecast integrations using the full ECMWF Integrated Forecast System model, using first the *OPERPROG* scheme, and then replacing this by the full nonlinear versions of *OPERDIAG* and *NEWDIAG* schemes in turn. This permits an assessment of the diagnostic schemes' physics relative to the operational forecast model, without invoking the additional errors associated with the tangent linear approximations. Finally section 6 assesses the validity of the tangent linear approximation of the new scheme before the conclusions are drawn in section 7.

2 The present 4D-Var Cloud Scheme

It is useful to summarize the salient features of the present 4D-Var diagnostic cloud scheme, outlined by Janisková et al. (2002b), before introducing the new scheme. The existing scheme is based on Slingo (1987), which was also used in the full forecast model prior to the implementation of current prognostic scheme of Tiedtke (1993). Slingo (1987) relates the cloud cover, C, to the grid-mean relative humidity (RH). As discussed by Tompkins (2002), a relative humidity approach implicitly assumes subgrid-scale fluctuations of vapour and cloud exist, without explicitly knowing the form of those fluctuations. The cloud cover is also adjusted according to the grid scale vertical velocity and convective precipitation (Slingo, 1987).

The in-cloud liquid water mass mixing ratio r_{cl}, is then taken as a fixed ratio of the saturation mixing ratio r_{sat}

(calculated according to Simmons et al., 1999), thus

$$r_{cl} = K r_{sat}, \tag{1}$$

where the constant K is currently set to 0.05. This crudely represents the vertical statistical relationship between cloud water (a term used for both liquid and ice) and saturation vapour pressure, which is by no means a strict relationship.

It is worth pointing out two features of this relationship. Firstly, the diagnostic determination of cloud water implies that it is not conserved between timesteps. This aspect will not change with the new scheme since it will also introduce a diagnostic cloud water equation. The second concern of the above in-cloud liquid water equation pertains to the temperature sensitivity. While roughly representing the reduction in cloud water with altitude, it reverses the observed horizontal relationship. If a physical process introduces a cooling in a cloud layer, Eq. 1 will subsequently reduce the in-cloud water content, while in fact the cooling and associated reduction in r_{sat} should lead to condensation. The reason this is not disastrous for the sensitivity of 4D-Var is because the grid mean liquid water r_l is given by $r_l = C r_{cl}$. The dependence of C on relative humidity usually, but not necessarily, implies an increase in grid mean cloud water in response to cooling. Despite the sign of the sensitivity being correct in most cases, this still implies that the magnitude is unlikely to be.

The treatment of rainfall is also problematic. This is determined by converting any supersaturation directly into rain, which falls out immediately. Rainfall evaporative processes currently inhibited. Rainfall bears no relation to cloud properties, except that neither can exist in very dry atmospheres, and clouds existing in subsaturated conditions are unable to form precipitation. This weakness is particularly prevalent in the tropics.

3 New 4D-Var Cloud Scheme

The new scheme can be divided into a number of components. The cloud cover and in-cloud liquid water content consists of two sources, stratiform and convective cloud, thus

$$C = C_{strat} + C_{conv}, \tag{2}$$

and similarly for cloud water. The stratiform and convectively detrainment cloud water are combined to derive the mean in-cloud water content, which is subsequently used to calculate the precipitation production. The precipitation flux is assumed to fall out within one timestep, and is allowed to evaporate during the descent. Each of these processes will be explained in turn.

Stratiform cloud properties

The new scheme is loosely based on statistical ideas, which assume a probability density function form to describe the subgrid-scale fluctuations of total water and/or temperature. This allows the in-cloud liquid water and cloud cover to be determined by integrating the saturated portion of the grid box. Examples of existing statistical schemes are given by Smith (1990), Bony and Emanuel (2001) and Tompkins (2002) and the reader is referred to these manuscripts for details of this approach.

Previous investigations have used a number of function forms to describe the PDF of subgrid-scale fluctuations, including symmetric triangular, uniform and Gaussian distributions (Sommeria and Deardorff, 1977, Smith, 1990, LeTreut and Li, 1991, Ricard and Royer, 1993), in addition to skewed forms such as the exponential, gamma and beta distributions (Bougeault, 1981, Barker, 1996, Tompkins, 2002), and in two instances bi-modal distributions (Lewellen and Yoh, 1993, Golaz et al., 2002). In this scheme, the simplest of all these

distributions is adopted, namely the uniform distribution, for a number of reasons. Firstly, the distribution is described by only two parameters, simplifying the closure task. Secondly, a number of the above distributions require iteration for their solution (see e.g. Tompkins, 2002) which is not desirable when the tangent linear or adjoint of the scheme is required. Simple distributions such as the triangular and uniform permit analytical cloud relations, although the triangular has the disadvantage of a discontinuous cloud cover relationship, which again can trigger stability issues in an assimilation context. The third and perhaps foremost reason for using the uniform distribution is for consistency with the full forecast model's scheme, which uses the same assumption for the clear sky vapour fluctuations (Tiedtke, 1993).

One of the two parameters specifying the uniform distribution can be determined from the control variables of temperature and humidity, combined to give the relative humidity. For the closure, a diagnostic assumption is made for the total water variance, or equivalently the distribution width. Knowledge of the relative humidity and the distribution width exactly specifies the uniform distribution and the cloud cover and water content can subsequently be diagnosed. As discussed by Tompkins (2002), if a fixed diagnostic relationship is used for the higher order moments of the distribution PDF, then the cloud cover can be directly derived as a relative humidity formulation. For example, assuming a constant distribution width for the uniform distribution of total water leads directly to the RH formulation of cloud cover used by Sundqvist (1978) and Sundqvist et al. (1989) which was later adopted by Lohmann and Roeckner (1996) and others.

It is likely that a constant variance is not accurate for all situations. Cloud can often form with low relative humidities, lower than 60% (Walcek, 1994), implying that often a wide distribution is required. However, using a fixed width distribution that forms cloud at $RH < 60\%$ renders unrealistically large values of liquid water as the relative humidity approaches saturation, since it does not take into account the effect that precipitation has in reducing distribution variance (Tompkins, 2002). The asymmetric nature of this process implies that a lower variance is required for high relative humidities, and this is included in an very simplified manner by reducing the distribution width linearly from its maximum value when $RH = RH_{crit}$, where RH_{crit} is a critical relative humidity for cloud formation, to its minimum value when $RH = 1$, which is determined by a constant parameter κ. The width of the uniform distribution W is given by

$$W = r_{sat}(1 - RH_{crit} - \kappa(RH - RH_{crit})), \tag{3}$$

which leads to the following relationship for the stratiform cloud cover:

$$C_{strat} = 1 - \sqrt{\frac{1 - RH}{1 - RH_{crit} - \kappa(RH - RH_{crit})}}. \tag{4}$$

The relationship between cloud cover and relative humidity is shown in Fig. 1 for various values of κ. When $\kappa = 0$, the relationship reduces to the form used by Sundqvist et al. (1989). Although this initial schemes uses a fixed distribution width, the use of a statistical scheme framework permits future development towards the use of a total water control variable. This could possibly be combined with a more complex but nevertheless diagnostic treatment of the variance equation along the lines of Lenderink and Siebesma (2000). Moreover, the knowledge of the subgrid PDF of water vapour fluctuations allows it to be used in other parametrizations consistently, such as the precipitation formulation, or as in the scheme here, the evaporation of precipitation.

In the same way, the knowledge of the PDF and its assumed variance leads to the formulation of the grid-mean cloud water mass mixing ratio which is given by

$$r_{l\,strat} = r_{sat} C_{strat}^2 (\kappa(1 - RH) + (1 - \kappa)(1 - RH_{crit})) \tag{5}$$

Thus it is clear that both the stratiform cloud cover and mass mixing ratio will be sensitive to the choice of the parameters κ and RH_{crit} which are defined as:

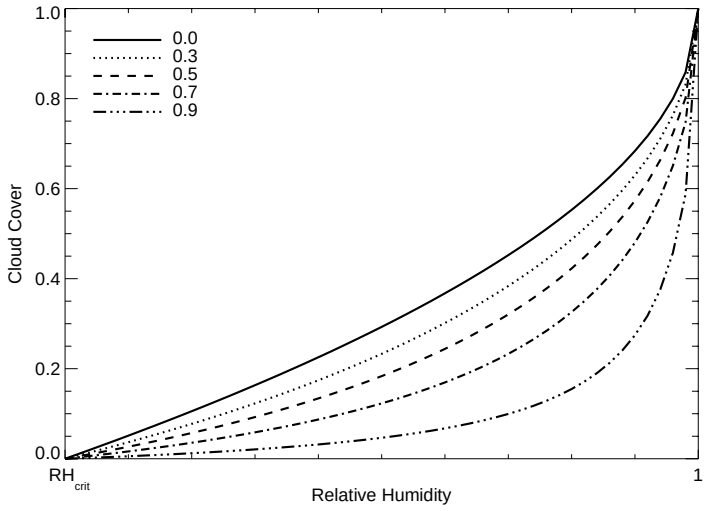

Figure 1: Cloud Cover versus relative humidity for various values of κ (see legend).

$$\kappa = MAX[0, 0.9(\sigma - 0.2)^{0.2}], \tag{6}$$

$$RH_{crit} = 0.7\sigma(1-\sigma)(1.85 + 0.95(\sigma - 0.5)), \tag{7}$$

where σ is the vertical coordinate of the pressure divided by the surface pressure. These functions are graphically depicted in Fig. 2, which shows the implemented profile of κ reduces from 0.86 through most of the lower troposphere towards zero in the upper troposphere. This, combined with the profile of RH_{crit}, implies that stratiform clouds are initiated at drier relative humidities in the mid troposphere and that the variance is largest at and above the tropopause region.

Convection contribution

One of the most significant sources of cloud in the tropics and mid-latitude summers in the Tiedtke (1993) cloud scheme is the detrainment from deep convection (e.g. Teixeira, 2001). Currently, the 4D-Var convection scheme does not provide such information, but this will be included in an improved scheme under development (Lopez and Moreau, 2003). The detrained cloud water is added to the diagnostic stratiform component given above. For the cloud cover, the assumption is adopted from Tiedtke (1993) that convective clouds randomly overlap existing stratiform cloud, and the source term is solved implicitly (after Eq. 37 in Tiedtke, 1993). Thus the convective cloud cover contribution (C_{conv}) is given by

$$C_{conv} = (1 - C_{strat})(1 - e^{\frac{-D\Delta t}{\rho}}), \tag{8}$$

where D is the mass detrainment rate, ρ is the density, and Δt is the timestep.

Unlike the prognostic Tiedtke scheme, no memory exists for cloud water between consecutive timesteps. Thus the additional assumption is made that any convectively detrained cloud water that is not converted to precipitation during the timestep, evaporates. This is necessary to prevent convectively active regions from artificially drying during the forward integration. It should also be noted that the present formulation is timestep dependent. As the timestep approaches zero the influence of convective detrainment is removed. Alternatively, an equilibrium solution for the cloud cover could be introduced, an approach complicated by the need to treat the

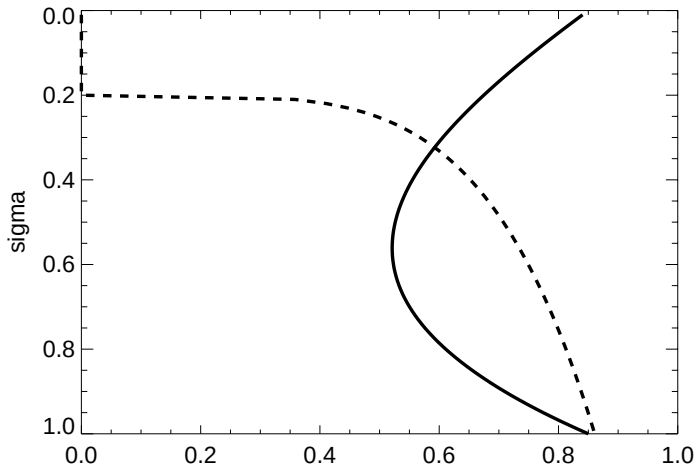

Figure 2: RH_{crit} (solid) and κ (dashed line)

cloud water consistently. This will investigated further, but the simple approach outlined here is retained for the initial implementation into 4D-Var.

Precipitation production

The generation of both snow and rain are parametrized as auto-conversion terms. The functional form adopted is based on Sundqvist et al. (1989) as

$$\frac{dr_l}{dt} = r_l c_0 \left(1 - exp\left[-\left(\frac{r_{cl}}{r_{cl}^{crit}}\right)^p\right]\right), \tag{9}$$

where r_{cl}^{crit} is the critical value of the in-cloud water content at which precipitation generation becomes efficient, set to 0.5 g kg^{-1}. The other variables c_0 and p are constants, given the values $3 \times 10^{-4}\Delta t$ and 2, respectively. Note that once the cloud water mass significantly exceeds r_{cl}^{crit}, the rate equation becomes quasi-linear, approximating $r_l c_0$. This behaviour replicates the Kessler (1969) scheme, but differs substantially from the power function forms adopted by, e.g., Beheng (1994) or Khairoutdinov and Kogan (2000). However, the nonlinearity of this adopted form at lower cloud mass mixing ratios still enforces the use of techniques to prevent instability when the tangent linear model is constructed, which will be outlined in detail below.

The local modifications of c_0 and r_{cl}^{crit} by Tiedtke (1993) to take into account the Bergeron-Findeisen or collection processes are not included here. Applying an autoconversion term for both snow and rain differs from the operational implementation of the prognostic Tiedtke (1993) scheme which was updated to include a treatment of ice sedimentation according to Gregory et al. (2000) and Jakob (2002). This is justified since it removes the discrete physic process transition existing in the latter. Auto-conversion forms the basis of snow generation in other more complex microphysical schemes (e.g. Lin et al., 1983, Brown and Swann, 1997) and also the original Tiedtke scheme. To compensate for the neglect of other processes in this simplified scheme, the liberty is taken to tune within reasonable limits the value of c_0, which is increased by a factor of three to obtain a sensitivity that reproduces as closely as possible the performance of the *OPERPROG* scheme.

Rainfall evaporation

As with the Tiedtke (1993) scheme, precipitation falls to the surface within one timestep and evaporates during its descent. To retain this important term, the new scheme also bases it on the Newtonian relaxation formulation of Kessler (1969) (see Eq. 35 of Tiedtke, 1993). However, there are some significant differences. Firstly, in the *OPERPROG* scheme, the precipitation fraction (the proportion of a grid cell through which precipitation is falling) is calculated via a maximum-random overlap assumption, similar to that used for the cloud cover in the radiation calculation (Jakob and Klein, 2000). For simplicity, the diagnostic scheme abandons this in favour of a maximum overlap assumption.

A second contrasting aspect of the new scheme is that it partially accounts for the overlap of precipitation with the subgrid clear sky distribution of humidity fluctuations, which we recall are uniformly distributed. Thus, instead of using the mean humidity throughout the whole clear sky region to calculate the rate at which rainfall evaporates, the new scheme uses the mean humidity only in the clear-sky portion through which the rainfall is falling, denoted C_{pre}^{clr}. Consistent with the maximum overlap assumption, this is taken to be the most moist C_{pre}^{clr} fraction of the clear sky. Using the uniform distribution,

$$r_{pre}^{clr} = r_{sat} - \frac{C_{pre}^{clr}(r_{sat} - r_v)}{(1-C)^2}. \tag{10}$$

The significant advantage of this new formulation is that it parametrizes the evaporative processes smoothly without switches or discrete transitions. In contrast, due to the lack of memory of subgrid scale fluctuations between timesteps, the operational Tiedtke (1993) scheme was forced to introduce a relative humidity threshold for rainfall evaporation to prevent eventual gridscale saturation. This threshold ranged linearly from 70% to 100% according to the precipitation fraction. If the initial RH exceeds this threshold, evaporation is completely inhibited, while if the RH is less than this threshold, the evaporation calculation is initially unimpeded, but is subsequently clipped, if necessary, to give the threshold value. This formulation not only introduces further (ad-hoc) tunable parameters to the scheme in the form of this threshold, but this approach, and in particular its numerical implementation, produces a noisy and discrete behaviour, undesirable for assimilation purposes.

The proposed scheme behaves smoothly, and replaces the tunable parameters with assumptions consistent with other model components. Moreover, despite the apparent differences, the new approach does not significantly alter the model climate. In order to demonstrate this, the new rainfall evaporation scheme was inserted into the Tiedtke scheme and tested for a 11 day analysis experiment, conducted at T511 resolution using model cycle 25r4 for June 2002. The Z500 scores over the 11 cases indicate little impact in both hemispheres (Fig. 3). For this period the new scheme appears to have a positive impact on the North American region (not shown) although extended tests are required to make more statistically robust conclusions for such a confined region. The impact on the 1000 hPa humidity is more notable, and the new scheme appears to improve the low level humidity in the extra-Tropics.

4 1D ARM Tests

The first attempt to validate the new scheme is in a semi-prognostic framework, similar to that used by Lord (1982). From each analysis at 00Z and 12Z, a 12 hour forecast using the full nonlinear *OPERPROG* scheme is conducted. In the 4D-Var system, such a forecast provides the trajectory calculation. The initial cloud state in the analysis system is provided by the first-guess trajectory forecast which was shown byJakob (2000) to remove the 10-12 hour cloud spin-up, and produce a smooth evolution of the cloud-related quantities. At each timestep of this short forecast the radiative statistics are compared to the available data from the Atmospheric

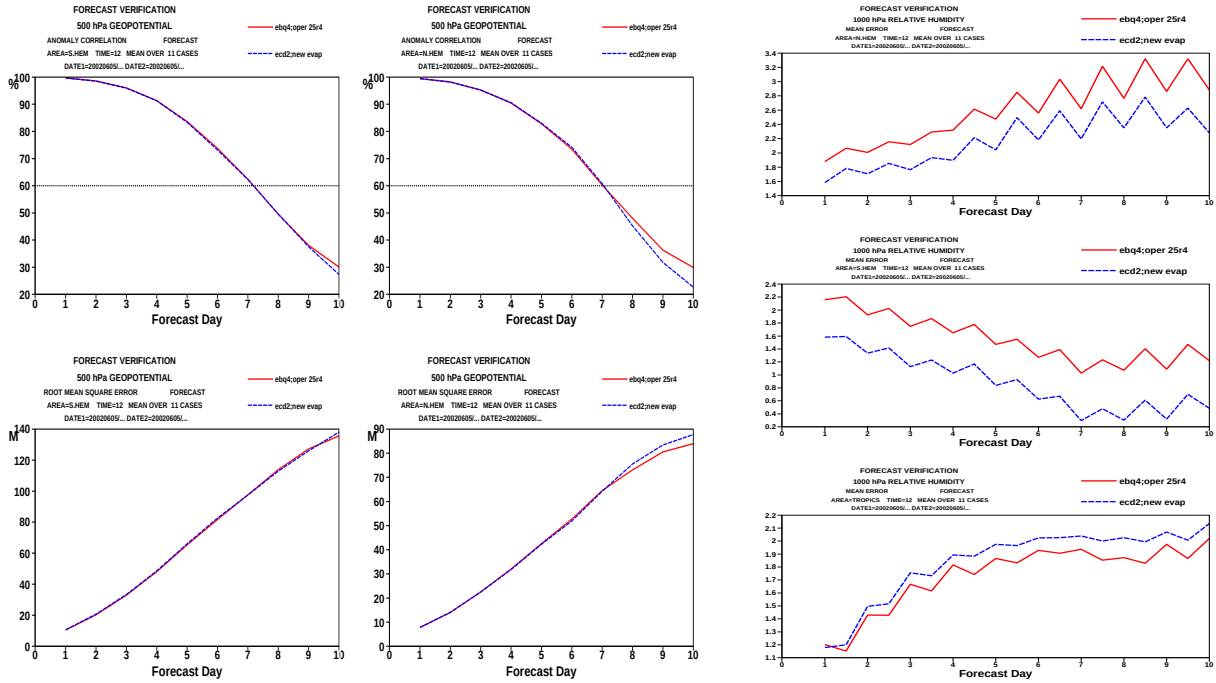

Figure 3: Left four panels: Z500 scores for 11 cycles of the default 25r4 forecast model (red lines) and the same forecast model with the new rainfall evaporation formulation (blue lines). Right three panels: 1000 hPa Humidity biases for northern and southern hemispheres and tropics

Radiation Measurement Program (ARM) sites[1], situated at Southern Great Plains (SGP) in North America, and the two tropics sites based at Nauru and Manus in the equatorial Western Pacific Ocean. Such a comparison has been previously conducted by Morcrette (2002), who provides details of the methodology.

The *OPERDIAG* and *NEWDIAG* cloud schemes are then tested in a semi-prognostic mode. This is done by taking at hourly intervals the control variables of humidity and temperature from the 'trajectory' forecast described above, and using these to drive the nonlinear version of each cloud scheme in turn. There is no feedback from the cloud schemes to the temperature and humidity fields; this initial test concentrates on the performance of the cloud schemes in a strongly constrained environment where the background thermodynamic fields are not permitted to diverge. In this way serious biases in the underlying cloud scheme physics may be identified. However, the strong constraints imposed by this methodology implies that it is unable to identify all deficiencies (e.g. long term drying or saturation of the atmosphere during a 4D-Var integration), and thus must be supplemented by alternative test procedures such as the full forecasts presented in section 5.

SGP site

The ARM Southern Great Plains (SGP) site is situated in Kansas and provides a wealth of cloud and radiation observations. The new diagnostic model is compared to the existing diagnostic model and the prognostic model. The cloud cover from each model is shown in Fig. 4 for the month of January, during which the majority of the cloud is most probably synoptically forced, rather than convectively generated. In such conditions, Walcek (1994) showed that relative humidity was a good predictor for cloud cover, and indeed, it appears that both diagnostic schemes produce similar cloud fraction evolution to the prognostic scheme. That said, OPER-DIAG tends to under-predict some of the mid-level and upper level clouds. This is a result of the relatively

[1] see www.arm.gov

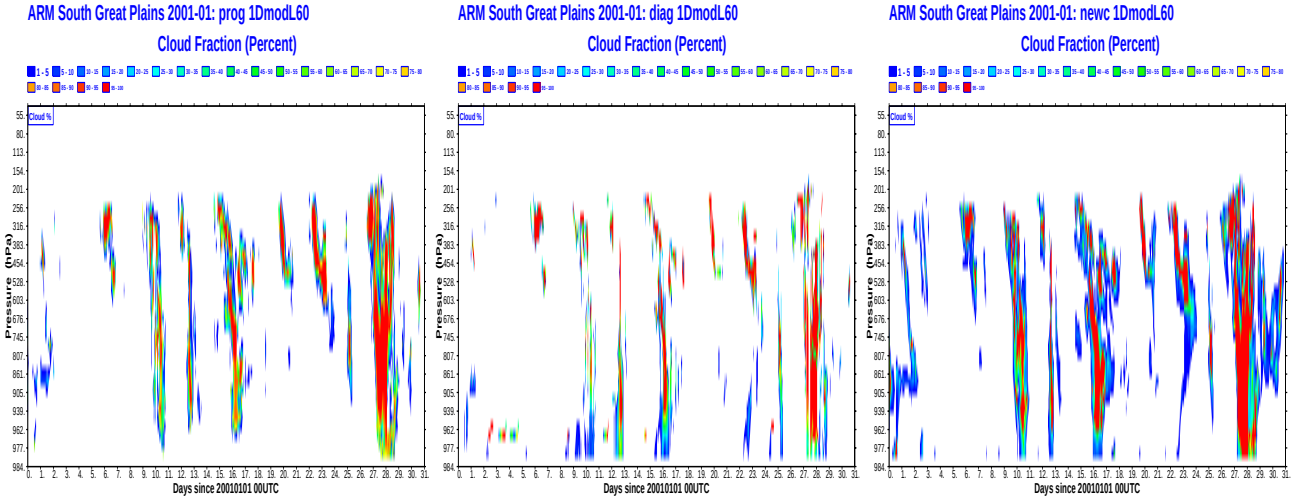

Figure 4: Cloud cover over the ARM SGP site during January 2001 predicted by the (left) Operational prognostic scheme (middle) 4D-Var operational diagnostic scheme, and (right) new diagnostic scheme. Contours are in 5% intervals.

high threshold of 80% relative humidity for the formation of clouds used in this scheme. Replacing this critical threshold by the profile used in the new scheme given in Eq. (7) leads to significant improvements in the prediction of synoptically forced mid-level clouds in the existing operational scheme (not shown).

In contrast, deep convection plays a significant role in generating cloud during the month of June at this location, and the new diagnostic model is obviously able to produce a more accurate fit to the prognostic model, due to its direct link through the detrainment term (Fig. 5). The operational model does make a number of artificial adjustments to the cloud fraction when deep convection is active, but these are not linked to the convective updraught properties. Thus, while the operational scheme may predict the occurrence of cloud in deep convective scenarios, the statistics are unlikely to reproduce the behaviour of the prognostic scheme. The short-comings of the existing scheme will be more apparent when the tropical sites are examined. Note that even with its direct link to the convection scheme, the new cloud scheme does not reproduce the longevity of the convectively associated cloud events. This is due to the use of a diagnostic rather than prognostic formulation for the convective cloud term, which only recognizes convection while it is currently active. The cirrus clouds that remain

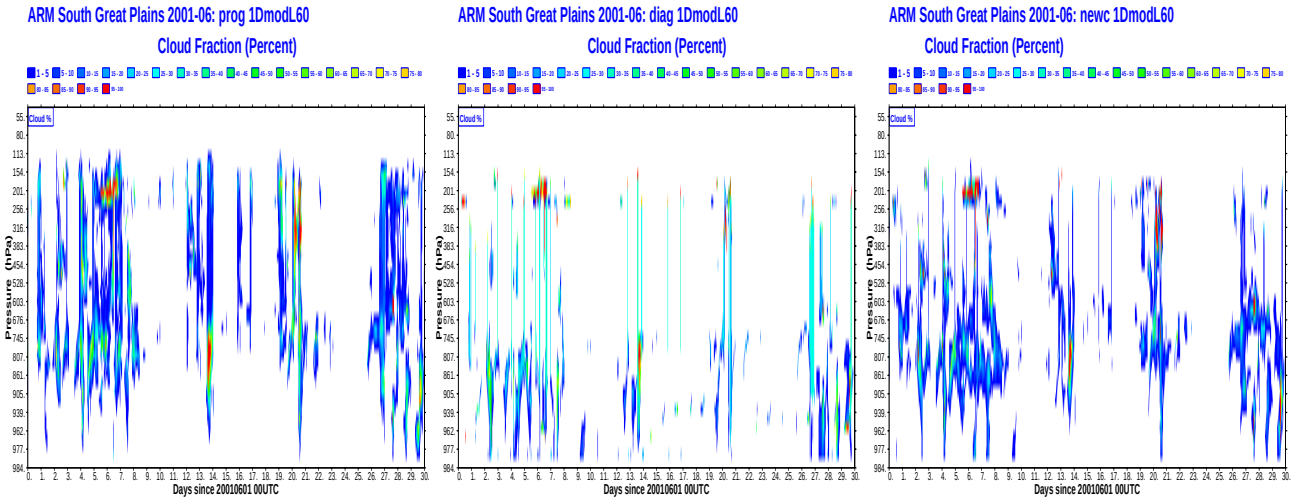

Figure 5: As fig 4 but for the month of June

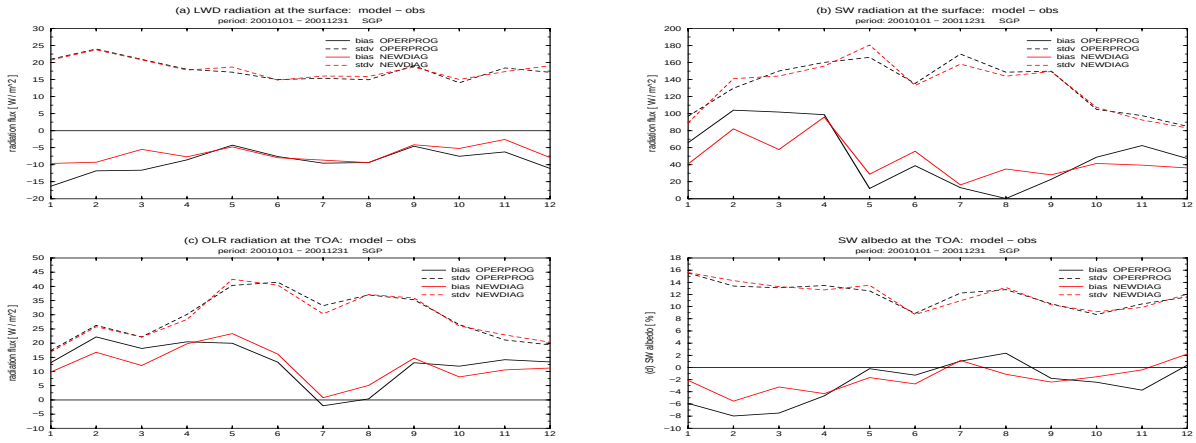

Figure 6: Monthly mean statistics for the year of 2001 for (a) Surface downward longwave, (b) surface net shortwave radiation, (c) TOA outgoing longwave and (d) shortwave albedo

in the prognostic scheme after the convection has died exist in a low relative humidity environment, rendering their accurate prediction by a diagnostic approach unfeasible. However, this dry environment also proscribes the persistence of these clouds, which evaporate rapidly, and thus the time-truncation of the diagnostic model represents a minor inaccuracy. If convection were to continue and moisten its environment to levels that prevent fast cirrus dissipation, then these would also be predictable by the diagnostic approach.

A comparison of the liquid water and ice mass mixing ratios for the January case, where the occurrence of cloud is well predicted, shows that both diagnostic schemes reproduce the ice and liquid water profiles of the prognostic model reasonable well, with the new diagnostic scheme giving less liquid and more cloud ice (not shown). In fact, the study by Chevallier and Kelly (2002) indicates that this increase of ice would bring the analysis closer to observations and is therefore beneficial.

The above comparisons showed detailed diagnostics for a particular month. To gain a more systematic view of the impact of the new scheme, Fig. 6 gives mean biases and root mean square errors in radiative quantities, calculated as a monthly mean for the whole of 2001. The observations used for the comparison are the net solar and infra-red fluxes at the top of atmosphere and surface. The TOA radiometric measurements are derived from geostationary satellite data (GOES-8 over the SGP site and GMS-5 over the tropical locations). This comparison is conducted for the new diagnostic scheme and the fully prognostic scheme, and shows that for all statistics, the new scheme gives a improved fit to the observations during winter, when cloud is mostly synoptically forced. When convective activity predominates during the late spring and summer months, the full prognostic scheme, with its ability to sustain anvil cloud in dry conditions, outperforms the diagnostic model. Overall, the two schemes are comparable, although it should be emphasized again that the thermodynamic fields are not free to evolve when using the diagnostic model.

Tropical sites

In addition to the SGP site, a comparison is conducted for the two ARM sites located in the tropical Western Pacific, at Nauru and Manus. These sites are located at 0.5S/167E and 2S/147E, respectively. Precipitation at these sites is convectively generated the whole year through, either from organised or isolated systems. It was seen from the SGP site statistics that these regimes pose the greatest difficulties for the diagnostic cloud scheme, and thus the tropical sites represent a more stringent test.

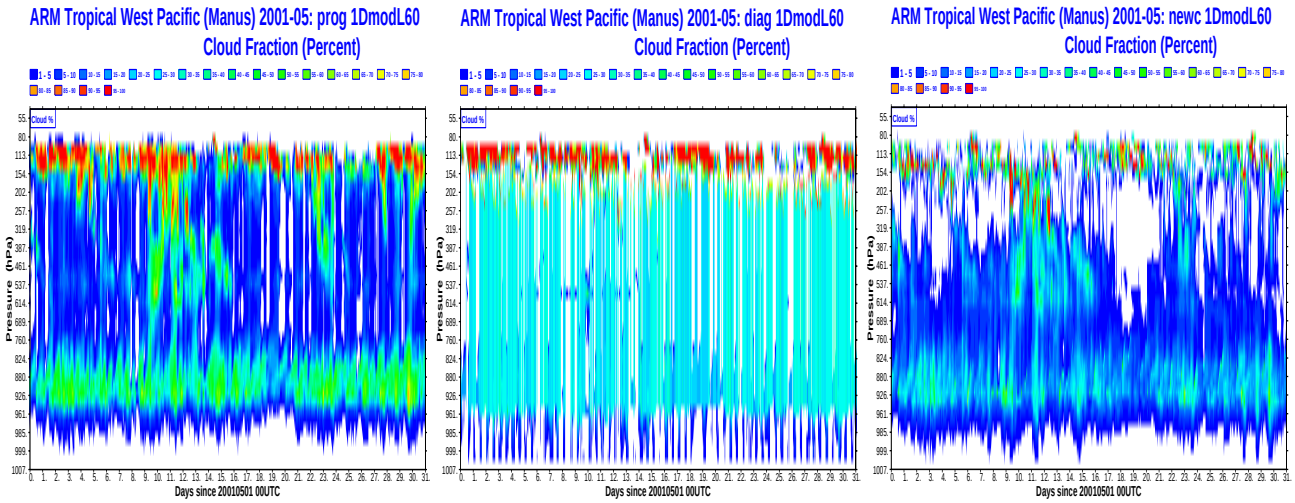

Figure 7: Cloud cover over the ARM TWP Manus site during May 2001 predicted by (left) OPERPROG (middle) OPERDIAG, and (right) NEWDIAG. Contours are in 5% intervals.

The simulations from the prognostic scheme shows that at both tropical sites the cloud is dominated by convective activity (figs. 7 and 8). There are two peaks in cloud cover, at around 900 and 100 hPa, corresponding to shallow and deep convection, respectively. The residual detrainment that occurs with the Tiedtke convective mass flux scheme (Tiedtke, 1989) also maintains a small residual cloud fraction throughout mid-levels, despite the dryness of the atmosphere there.

The new cloud scheme is unable to maintain these small mid-tropospheric cloud amounts in the presence of low humidities. However, the scheme is able to reproduce the general cloud fraction structure well, with peaks in the lower and upper cloud fractions. As for the ARM SGP site, the upper level cirrus is less continuous, again due to the lack of memory for the convectively enhanced cloud from one timestep to the next. The nature of the semi-prognostic test, where the temperature and humidities are continually reset, exacerbates these discrepancies. The evaporation of the detrained cloud water would lead to a moistened upper troposphere and eventually an increased cloud cover. This cirrus anvil cloud appears to be better represented in the existing operational diagnostic scheme, where the cloud cover at the uppermost detrainment level is artificially enhanced

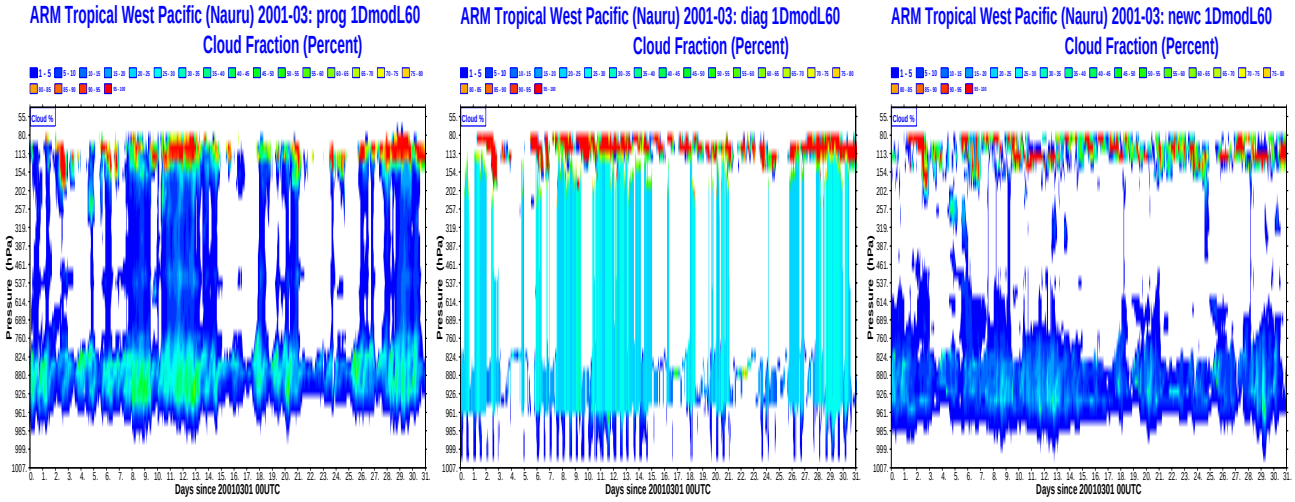

Figure 8: As fig 7 but for the ARM TWP Nauru site during March 2001

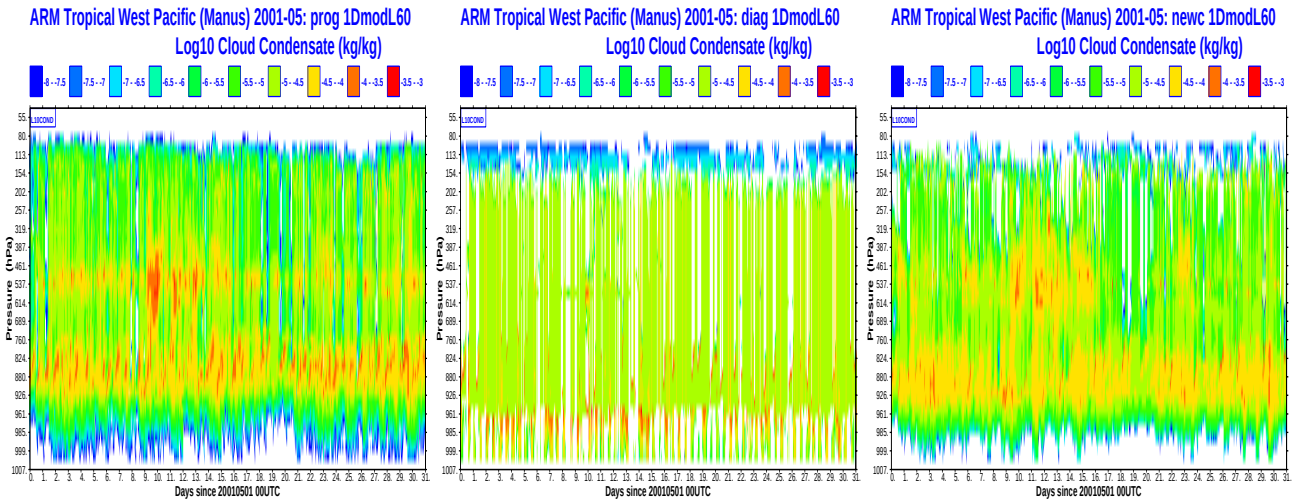

Figure 9: As Fig. 8 but for cloud (ice+liquid) mass mixing ratio

in the presence of deep convection according to Slingo (1987). The cloud cover throughout the mid-troposphere is a fixed function of convective precipitation amount, which mostly produces a value of around 30% in these cases, producing a strong and erroneous peak in the relative humidity/cloud cover PDF (not shown). The cloud cover does not respond to the evolving thermodynamic conditions in a reasonable way and it is apparent that the lack of shallow convection and the erroneous boundary layer cloud are problematic features. The sum of the liquid and ice mass mixing ratio for the Manus site are shown in Fig. 9, revealing that the new scheme produces an authentic replication of the prognostic scheme's profile of both ice and liquid, with the peak in mid-level liquid also present. Although the models are close, the new diagnostic scheme produces less liquid water and more ice than the prognostic scheme, which is in fact a global feature. In comparison to *NEWDIAG*, the present operational diagnostic scheme is obviously deficient.

5 Global Forecasts

The semi-prognostic tests described in the previous section give a brief insight into the operation of the two diagnostic schemes, given the caveat that the humidity and temperature fields are not free to evolve. A more stringent test, therefore, is to conduct full integrations of the ECMWF forecast model, substituting the prognostic cloud scheme by *OPERDIAG* and *NEWDIAG* in turn. The nonlinear versions of the diagnostic cloud schemes are used since the aim is to evaluate the cloud physics, and not the validity of the linear assumption.

Two weeks of forecasts are conducted at T159 resolution. The statistics are examined at a forecast range of 12 hours, which is the current assimilation window of 4D-Var. This choice of resolution and integration length therefore mimics the current inner-loop integration of 4D-Var. The initial conditions for the cloud field and other thermodynamic variables are interpolated from the T511 resolution operational analysis. As stated earlier, the cloud fields in the analysis are taken directly from the 'first-guess' trajectory forecast using the *OPERPROG* scheme. Therefore the global forecasts conducted using the two diagnostic schemes are likely to undergo an initial period of adjustment, often termed 'spin-up'. However, Mahfouf et al. (1999) and Jakob (2000) effectively demonstrated that cloud fields equilibrate after approximately 10 hours, and thus by examining the forecast range of 12 hours the cloud statistics are mostly unaffected by the initial state.

The total cloud cover for the forecast integrations (Fig. 10) reveals a marked correspondence between the new cloud scheme and the prognostic scheme, both for the mid-latitude and tropical regions. In most areas the lo-

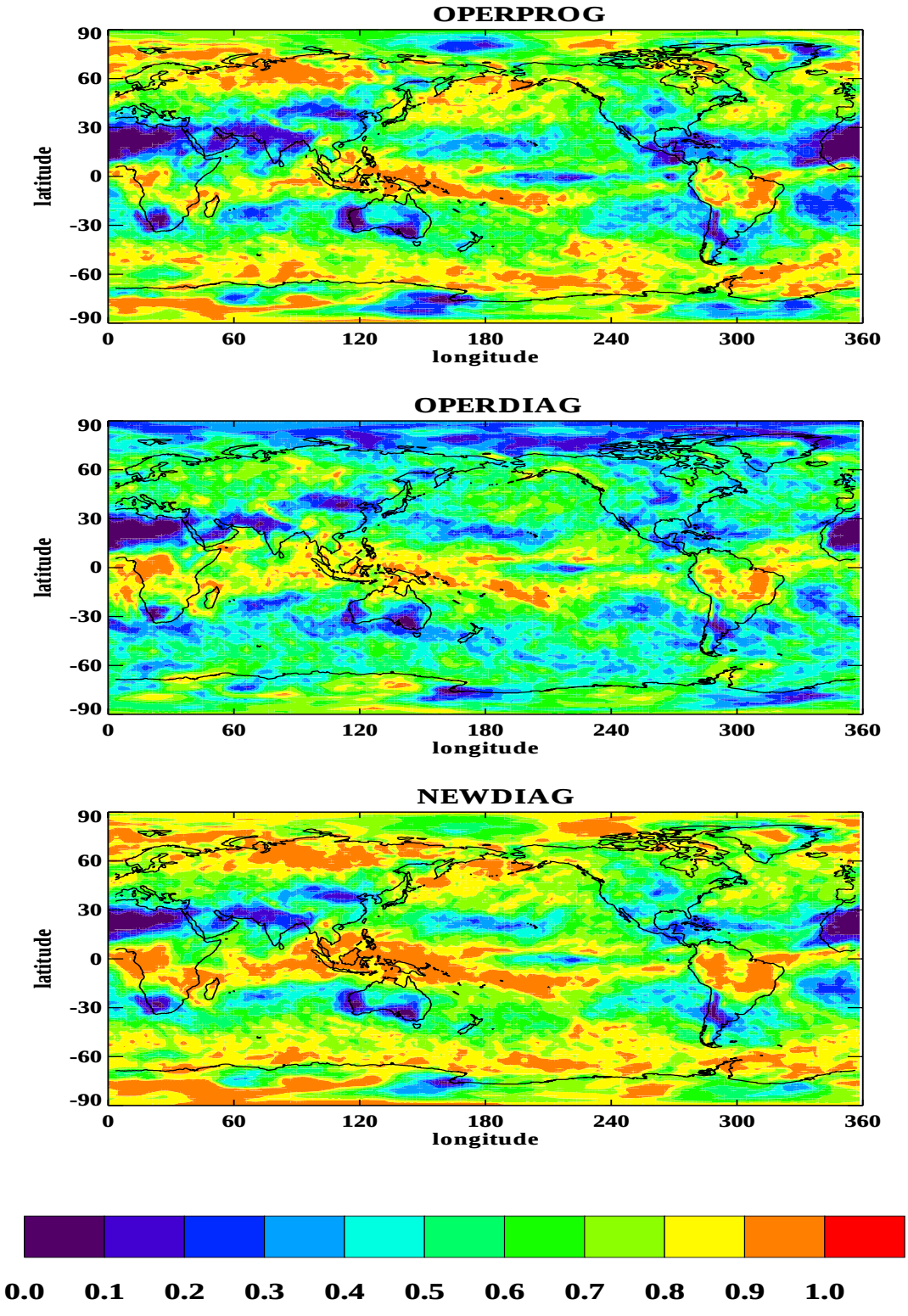

Figure 10: Instantaneous total cloud cover averaged over 14 forecasts at T159 resolution at the 12 hour range for (top) OPERPROG, (middle) OPERDIAG and (bottom) NEWDIAG

cation and amount of cloud are captured well. Closer examination indicates that *NEWDIAG* produces a higher cloud amount than *OPERPROG*, especially in the tropics. This contrasts to the findings of the previous section, which highlights the limitations of the semi-prognostic test and also the potential dangers of generalizing the conclusions drawn from localized gridpoints. Although the current operational diagnostic scheme also does a reasonable job at predicting the location of clouds, the amount is significantly underestimated, particularly in mid-latitudes. Note that neither diagnostic scheme is able to compensate for the deficiencies of the operational forecast model, such as the lack of stratocumulus regimes over the coast of the Americas (Jakob, 1999).

The strength of the new diagnostic scheme is revealed when maps of precipitation are examined (Fig. 11). Both *OPERDIAG* and *NEWDIAG* are able to faithfully mimic the Tiedtke scheme in mid-latitudes. This is quite surprising when the simplicity of *OPERDIAG* is considered, where precipitation is simply the result of removing supersaturation over one timestep. However, the operational diagnostic scheme evidently suffers catastrophic failure in the tropics, producing almost no precipitation. The *NEWDIAG* scheme is able to also convincingly reproduce the tropical precipitation, although the area coverage of precipitation appears to be larger, with many areas receiving small but non-negligible amounts of rainfall. This latter difference may be the result of the revised evaporation formulation in the diagnostic scheme, and has implications when used in 1DVAR assimilation techniques (Moreau et al., 2003).

The final figure examines the total column cloud water for the three cloud schemes at the same 12 hour range. The existing scheme *OPERDIAG* clearly produces too little cloud condensate in mid-latitudes, while cloud water is widespread through out the tropics. The new diagnostic scheme better predicts the location of the cloud water, and as with the other variables, the *NEWDIAG* is found to match *OPERPROG* more closely. The peak cloud water contents in the extra-tropics match well. It is notable that the new scheme does increase the cloud water in some areas of the tropics, which is due to an increase in upper level ice cloud with respect to the Tiedtke scheme (not shown). It is arguable that this is beneficial since previous investigations by Chevallier and Kelly (2002) indicate that the *OPERPROG* scheme produces too little upper level ice.

The forecasts were also examined at a range of 24 hours, to verify that the conclusions drawn would be robust if the assimilation window were to be extended in the future. No significant departure in the forecast behaviour were noted at this extended range and the results are not shown for reasons of brevity. Note that the validity of the linear approximation at these ranges was not tested, and is likely to be a limiting factor for such nonlinear processes.

6 Validation of the Linearized Scheme

The linearized versions (tangent-linear and adjoint) of the described cloud scheme have been developed. After the standard validation of the tangent-linear and adjoint codes (Taylor formula and adjoint identity), the linear evolution of the model with new cloud parametrization has been studied. Since for practical applications the utility of tangent-linear (TL) and adjoint (AD) models is determined by how well they describe the behaviour of finite-size perturbations corresponding to ones in the nonlinear model, the accuracy of the linearization of cloud scheme is studied with respect to pairs of nonlinear results as in Janisková et al. (2002a). Comparisons are then made between the evolution over 12 hours of analysis increments $\delta\mathbf{x}$ ($\delta\mathbf{x} = \mathbf{x}^a - \mathbf{x}^b$, where $\mathbf{x}^a$ represents analysis and $\mathbf{x}^b$ background field) with the simplified tangent-linear model $M'(\delta\mathbf{x})$ and the finite differences between two nonlinear forecasts ($M(\mathbf{x}^a) - M(\mathbf{x}^b)$) using the full nonlinear physical package, starting from the different initial conditions. Experiments are performed for three cases to sample the seasonal cycle (15 December 2000, 15 March 2001, 15 June 2001) using the model resolution T159L60 (120 km horizontal resolution and 60 vertical levels) of the ECMWF global spectral model, mimicking an inner-loop integration of the operational 4D-Var system.

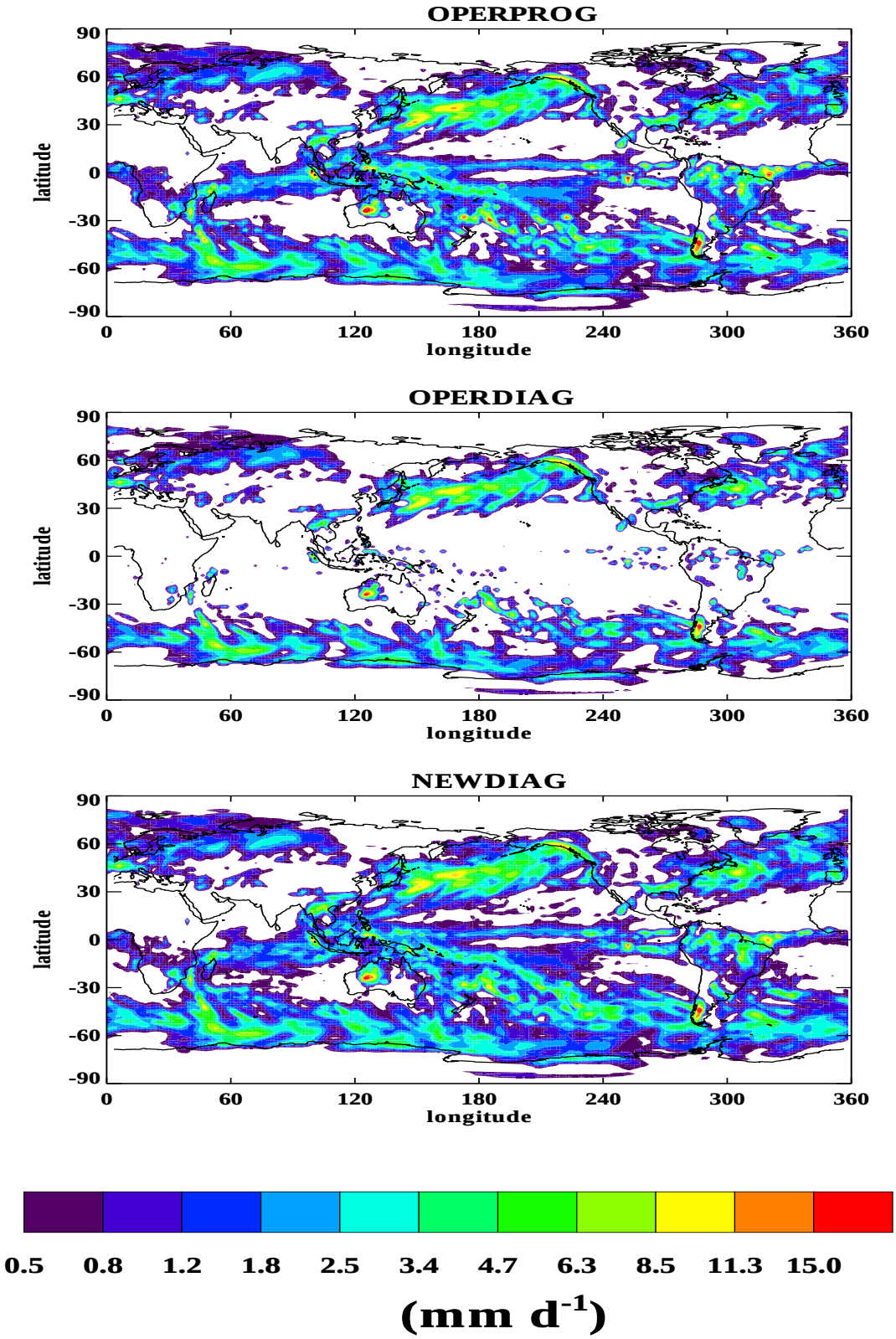

Figure 11: As Fig. 10 but for 12 hour accumulated large-scale precipitation

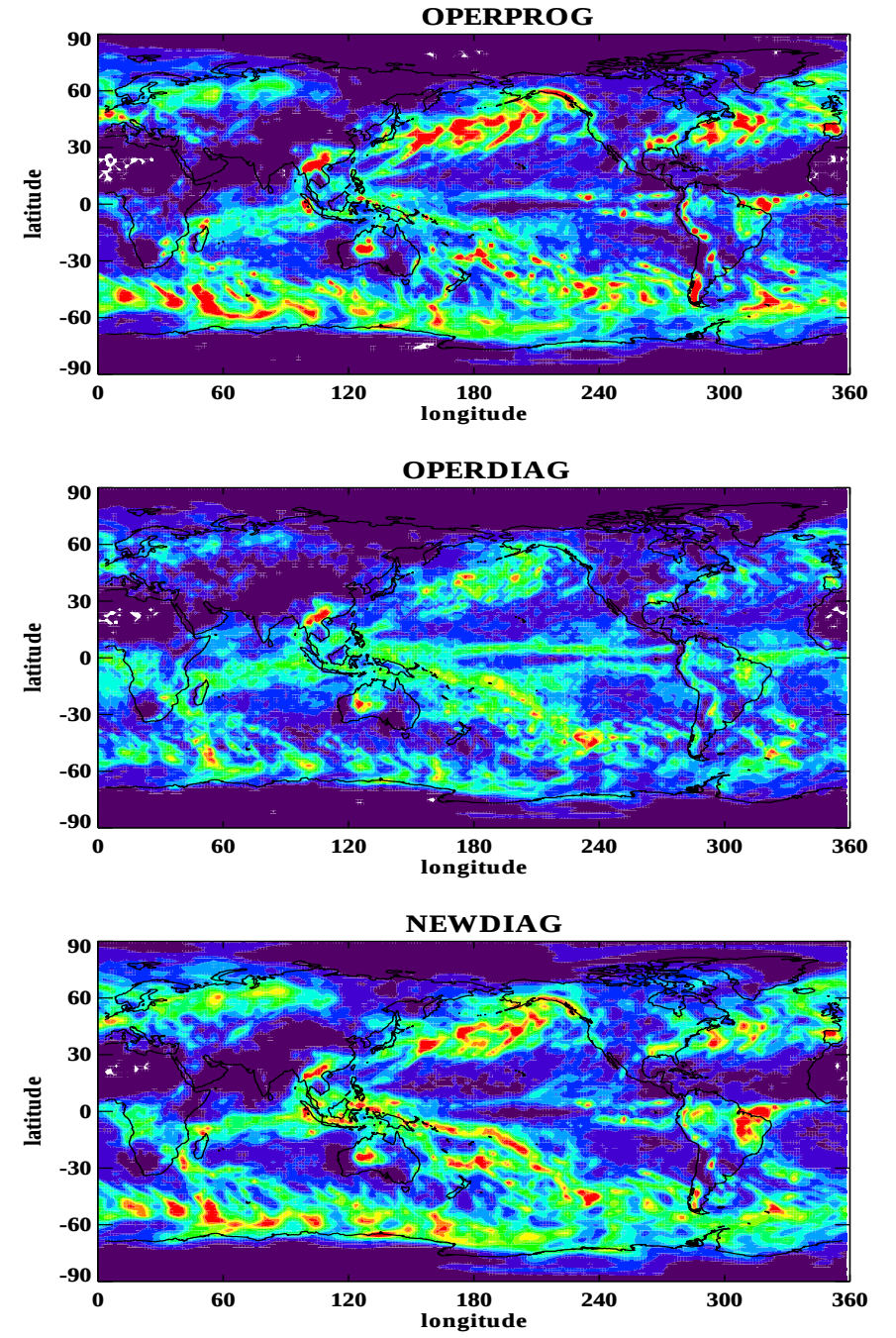

Figure 12: As Fig. 10 but for total column cloud water (liquid + ice)

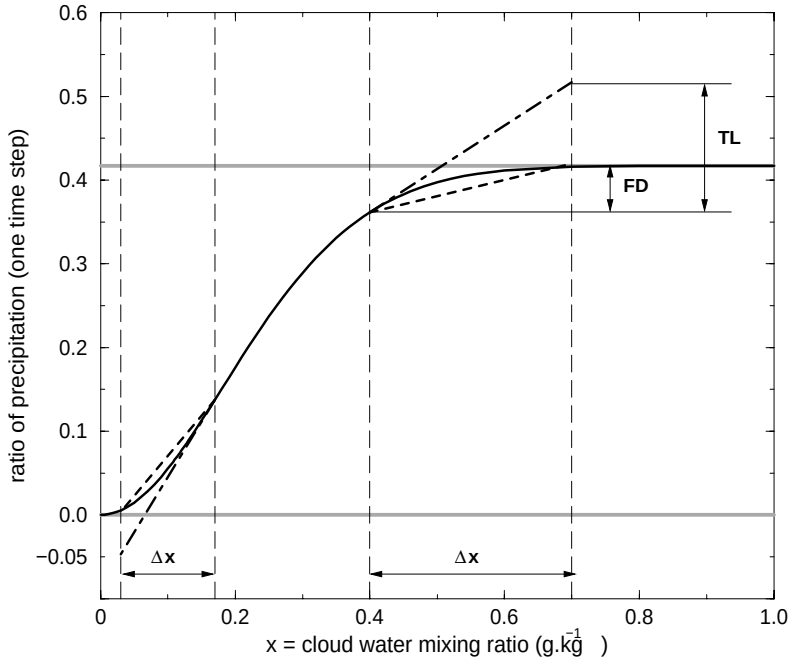

Figure 13: Regularization for the auto-conversion function F of cloud water into precipitation: Function describing which portion of cloud water mixing is converted into precipitation in one time step (black solid line), the physical limits of the function: 0 and 0.417 (grey solid line), the original tangent to the function for a given change in the cloud water Δx (dot-dashed line) and the proposed approximation for the linearized model (thick dashed line). FD indicates the size of finite difference increment ($F(x+\Delta x)-F(x)$) and TL is used for the tangent-linear increment $F'(\Delta x)$.

Regularization of the tangent-linear scheme

Initial investigations showed that the linearized scheme developed noise during the integration, despite the efforts expended to produce a smooth and differentiable parametrization scheme. A detailed post-mortem revealed a sensitivity to the auto-conversion function describing the conversion of cloud water to precipitation. From Eq. 9, the amount of cloud water converted to precipitation over one timestep is given by

$$F = 1 - exp\left\{ -c_0 \cdot \left(1 - exp\left[-\left(\frac{r_{cl}}{r_{cl}^{crit}}\right)^2 \right]\right) \right\} = 1 - exp(-R). \tag{11}$$

This function has two physical limits, which constrain the amount of created precipitation to be between zero and $1 - exp(-c_0)$ (grey lines in Fig. 13). In the TL model, any conditional decision is taken according to the trajectory (nonlinear model) around which the linearized model evolves. It is therefore a possibility that the linearized model will exceed physically reasonable limits. Such a circumstance is demonstrated in Fig. 13 by dot-dashed lines, where the perturbation of cloud water Δx creates a TL increment exceeding both the nonlinear one ($F(x+\Delta x)-F(x)$), and the physical limits defined by the trajectory. Such excessive increments can then lead to the development of noise in the time integration of the linearized model.

One solution of the problem would be to change the power $p = 2$ in Eq. 9 to make the function smoother and less steep. However, experiments showed that such modification simply postpones the development of noise and can

deteriorate the quality of the physical parametrization itself. Another possibility is not to allow an increment $R' = \partial R/\partial r_{cl}$, when added to the basic state R, to exceed the physical limits defined by the parametrization scheme. This means ensuring that $R + R'$ is not smaller than zero or larger than c_0. Such a control can be implemented in the TL model by introducing a weighting factor, which is equal to 1 when $R + R' > 0$ or $< c_0$ and has a value in the interval [0,1] otherwise. The proposed approximation is displayed in Fig. 13 by dashed line. It is obvious that the linearized scheme is consequently not the exact tangent-linear version of the cloud scheme. However, this is already a case for many smoothing modifications applied in the linearized models with physical parametrization schemes (for instance, neglecting or reducing the size of perturbation of exchange coefficients in the vertical diffusion schemes, such as in Mahfouf, 1999, Janisková et al., 1999, Laroche et al., 2002). Such a solution can also be applied since the incremental formulation of 4D-Var used at ECMWF (Courtier et al., 1994), for which the parametrization scheme was mainly developed, allows one to use a simplified model which does not need to be exact tangent-linear version of the nonlinear model (using lower resolution, simplified physics and so on). The modified scheme remains linear, and its adjoint can be constructed providing that the weighting factor w_a computed during the TL integration is saved for each grid point and model level. The weighting factor is computed as:

$$w_a = \begin{cases} \frac{c_0 - R}{R'} & \text{if } R + R' > c_0 \\ \frac{-R}{R'} & \text{if } R + R' < 0 \\ 1 & \text{otherwise} \end{cases} \tag{12}$$

The original value of R' is then replaced by $w_a \, . \, R'$ where w_a is treated as a constant for the linearized model, though varying according to the different conditions. After applying the described modification, the linearized scheme does not create any noise in the TL evolution of increments.

Results of the validation experiments

In the following evaluations, the impact of the cloud scheme is examined using mean absolute errors between the tangent-linear and nonlinear integrations as:

$$\varepsilon = \overline{[M(\mathbf{x}^a) - M(\mathbf{x}^b)] - M'(\mathbf{x}^a - \mathbf{x}^b)} \tag{13}$$

where M is the forecast model starting either from the analysis $\mathbf{x}^a$ or from the background $\mathbf{x}^b$ and M' is the tangent-linear model starting from the initial conditions $\mathbf{x}^a - \mathbf{x}^b$. The results are evaluated as a relative impact (in %) as:

$$\eta = \frac{\varepsilon_{exp} - \varepsilon_{ref}}{\varepsilon_{ref}} \, . \, 100 \, \% \tag{14}$$

where ε_{exp} and ε_{ref} are absolute mean errors for experimental and reference runs, respectively.

Figure 14 summarizes the relative impact η of the new diagnostic cloud scheme for temperature, specific humidity and zonal wind. In this figure, ε_{ref} represents the absolute mean error of the TL model using the set of operational linearized physics combined with the radiation schemes (*new_rad*) described by Janisková et al. (2002b). The experimental run (*new_rad_cloud*) includes the linearized version of the new cloud scheme. The results are presented for various geographical domains. Including the cloud scheme in the linear model improves globally the fit to the nonlinear model for each evaluated variable. The largest improvement is achieved in the Tropics for temperature and zonal wind and in North20 for specific humidity. A small negative impact is mainly observed for zonal wind in North20. The ability of the TL model to approximate the finite differences will necessarily be

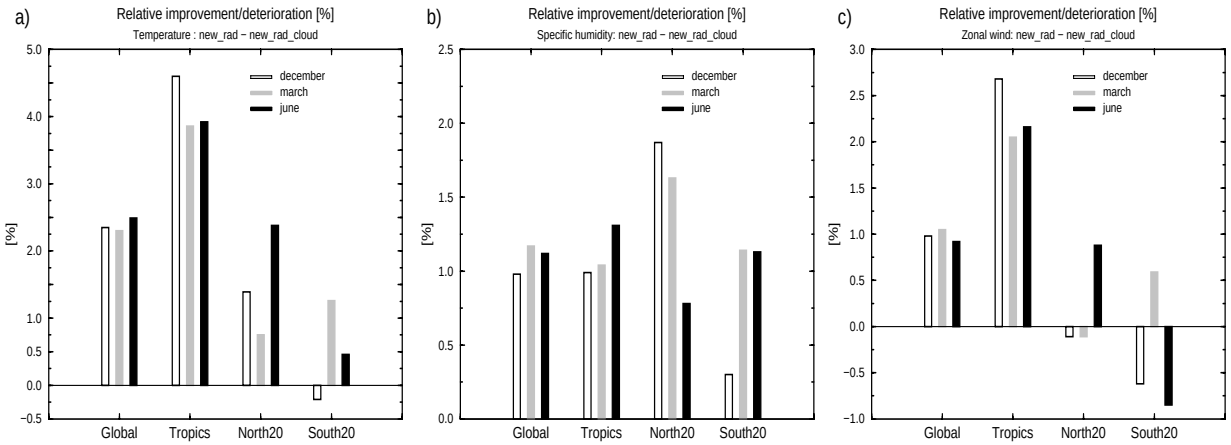

Figure 14: The improvement/deterioration of the tangent-linear (TL) model when using the new linearized cloud scheme in place of the current operational diagnostic scheme for the geographical domains of: Tropics: 20N-20S, North20: 20N-90N, South20: 20S-90S and globally. The results are presented as the percentage improvement for (a) temperature, (b) specific humidity and (c) zonal wind. The comparisons are made for 15 December 2000 (white bar), 15 March 2001 (grey bar) and 15 June 2001 (black bar).

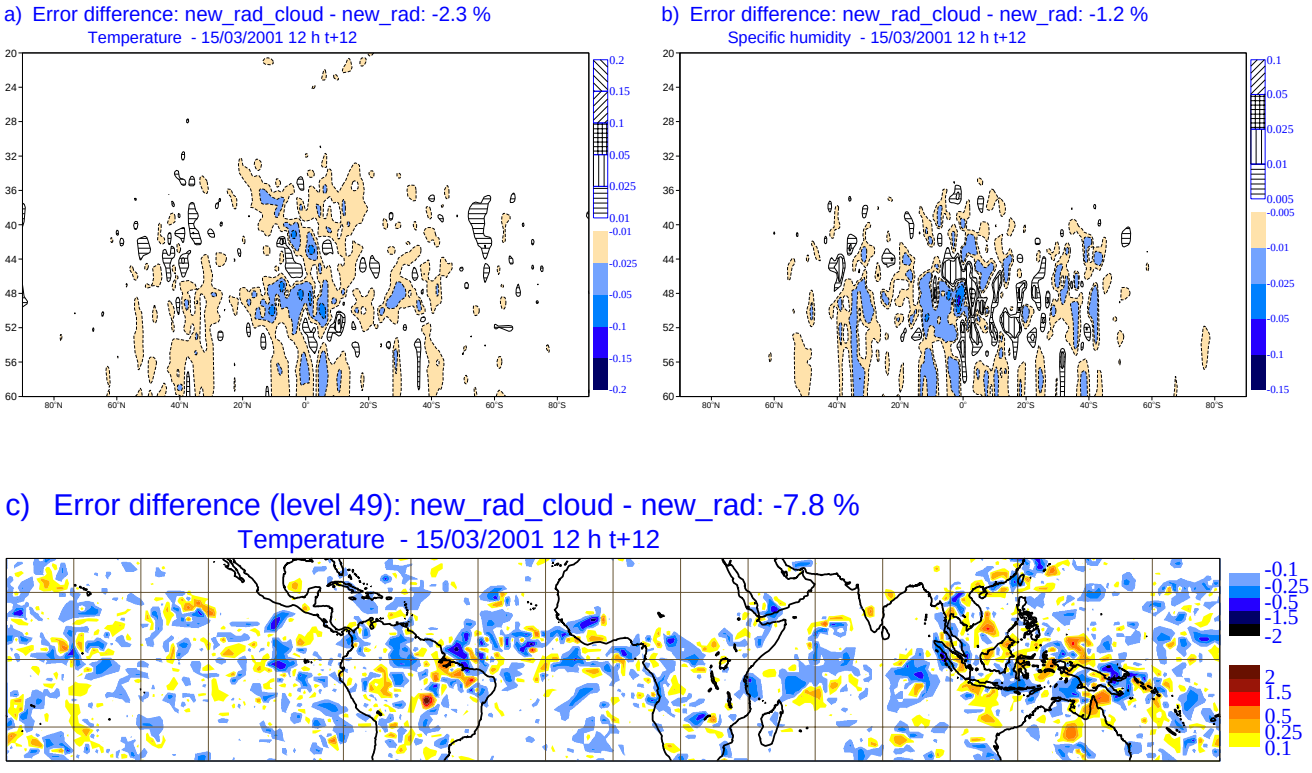

Figure 15: Influence of the tangent-linear (TL) cloud scheme on the evolution of temperature (a) and specific humidity (b) increments in zonal mean. Results are presented as the error differences (in terms of fit to the nonlinear model with full physics) between the TL model with operational linearized physics including new radiation schemes and the TL model with new cloud and radiation schemes. (c) presents the same, but for temperature at the model level L49 (∼ 850 hPa) and in the tropical domain (30S - 30N). 12-hour forecast for the situation of 15 March 2001, 12 UTC, units: K for temperature, $g.kg^{-1}$ for specific humidity.

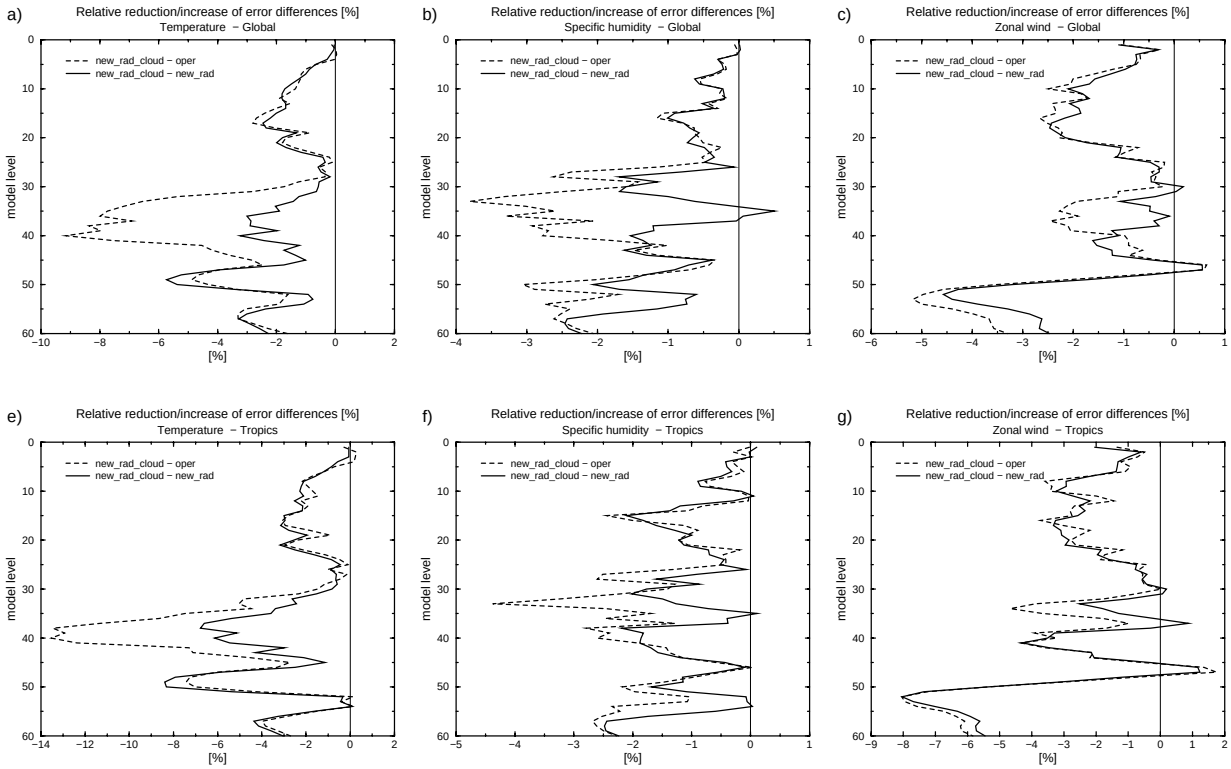

Figure 16: Vertical profiles of relative decrease (negative values) or increase (positive values) of error differences as a percentage for temperature (a,e), specific humidity (b,f) and u wind component (c,g). Results are shown for global statistics (top panels) and only the Tropics (bottom panels). The dashed line compares the combined package of the new radiation and cloud schemes to the operational set of the linearized physics. The solid line shows the impact of adding the new cloud scheme to the new radiation scheme. These results are for the 12-hour forecast on the 15th March 2001, 12 UTC.

dependent on the meteorological situation, but generally the largest improvements are generally in the Tropics, with the exception of specific humidity for which the improvement is globally uniform.

For a detailed presentation of the impact coming from the cloud scheme, zonal mean values of error differences ($\varepsilon_{new\_rad\_cloud} - \varepsilon_{new\_rad}$) are displayed in Fig. 15 for temperature and specific humidity, just for the situation of 15 March 2001. Negative values are associated with an improvement of the experimental TL model (*new_rad_cloud*) with respect to the reference one (*new_rad*) since they correspond to a reduction of the error ε. The new cloud scheme reduces the global mean error by 2.3 % for temperature and by 1.2 % for specific humidity. The improvement is significant over the whole Tropics and in the lower troposphere, as demonstrated in Fig. 15c, which presents error differences for temperature at the model level L49 ($\sim$ 850 hPa) in the tropical domain (30S - 30N). At this level the relative improvement is as large as 7.8 %, despite the fact that the TL integration was performed with a simple convection scheme (i.e., no perturbation of the detrainment term), since the new scheme can generate precipitation when the relative humidity is less than 100 %. The areas of error reduction correspond to the regions with the most improvement observed in the 3D forecast validation (section 5). Further improvements are expected when the scheme will be combined with the new linearized convection scheme recently developed (Lopez and Moreau, 2003).

Figure 16 showing the vertical profiles η (Eq. 14) of relative reduction or increase of error differences provides a more detailed examination of the influence of the *NEWDIAG* scheme on the vertical profiles, both globally and for the Tropics only. Results are presented for the combined new radiation and cloud schemes compared to the operational set of the linearized physics to demonstrate the impact of cloud-radiation interaction processes.

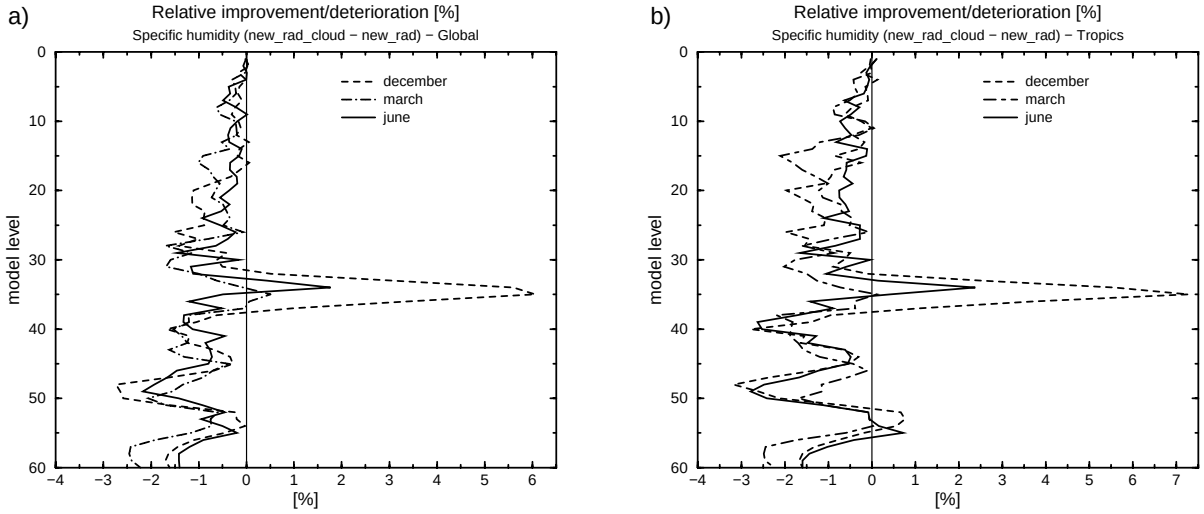

Figure 17: As solid line curves on Fig.16, but only for specific humidity, globally (a) and in the Tropics (b) and for the different situations: 15 December 2000 (dashed line), 15 March 2001 (dot-dashed line) and 15 June 2001 (solid line).

The new cloud scheme is also analysed in isolation. The impact of cloud-radiation processes is largest between the model levels L35 to L41 ($\sim$ 350 - 600 hPa) for temperature (improvements between 8 to 10 % globally and 10 - 14 % in the Tropics) and for specific humidity (improvements between 3 - 4 % globally). For the zonal wind, the error is mostly reduced below the model levels L48 - L49 ($\sim$ 800 hPa). The solid line indicates that it is the cloud scheme that produces this positive impact for humidity. The impact of the cloud scheme on temperature is smaller than that of the radiation scheme between L35 - L41, but its influence dominates below L49 ($\sim$ 850 hPa). It is probable that evaporation processes, which were neglected in the previous version of the linearized large-scale condensation scheme (Mahfouf, 1999), contribute to this error reduction when using the new cloud scheme.

There is an increase in error differences for specific humidity at L31 - L34 ($\sim$ 200 - 300 hPa), where the absolute mean error ε (not shown) is quite small (0.02 - 0.03 g.kg^{-1}). As seen from Fig. 17 displaying the vertical profiles of relative error reduction/increase for specific humidity in the different situations, this deterioration is general and is most significant for the winter case. This is likely to be a result of differing ice microphysics used in the two schemes. The lower end of the peak marking the deterioration is at exactly the temperature (250 K) at which the operational prognostic scheme discretely switches its physics from the Sundqvist-based auto-conversion for the mixed phase, to a sedimentation-based form for the pure ice phase. The new diagnostic scheme, using auto-conversion throughout the troposphere to ensure a smooth scheme, is unable to reproduce the behaviour caused by this discrete change in physics.

Detailed analysis of the results has shown that, except for the isolated deterioration described above, the inclusion of cloud scheme within existing linearized parametrizations improves overall the accuracy of the tangent-linear approximation of the simplified model to the full nonlinear model (in finite differences).

7 Conclusions

A new cloud scheme has been developed specifically for the purposes of variational data assimilation; a task complicated by the inherent nonlinearity of many cloud processes. The attempt was made to develop a scheme which is simple and does not contain discrete transitions, while retaining the central aspects of the Tiedtke scheme used in the nonlinear forecast model.

The new model diagnoses cloud cover and cloud water (liquid+ice) from the input profiles of the temperature and humidity control variables. This is performed in the spirit of statistical cloud schemes by assuming a subgrid distribution for the fluctuations of humidity. The uniform distribution is chosen for coherency with the full prognostic cloud scheme. Currently the variance of the distribution is fixed, implying that the cloud cover and liquid water can be reduced to formulations based on relative humidity. This statistical framework is flexible for future development, and will facilitate the move to a total water variable, if this is deemed to be advantageous for the assimilation system.

Simple auto-conversion terms are used for the generation of rain and snow, which fall out of the model column during one timestep. One novel aspect of the scheme is a new treatment of precipitation evaporation during the descent, which takes the subgrid-scale distribution of humidity into account in a self-consistent fashion. This new treatment removes the requirement of artificial and discrete process thresholds used in the full prognostic model, which would impact the feasibility of the tangent linear code.

The scheme is tested by examining physical tendencies of thermodynamical quantities over a series of timesteps given fixed input profiles of temperature and humidity. This is conducted over three sites in North America and the Tropical Western Pacific, and the new diagnostic scheme is found to give comparable results to the full forecast model for radiation and cloud observations. As a further test, a series of model integrations were executed, with the full prognostic scheme used in operational forecasts replaced in turn by the nonlinear versions of the current operational assimilation diagnostic cloud scheme, and then by the new scheme described here. Using the default model as a metric, the new scheme improves on the current assimilation cloud scheme for many variables such as cloud cover and ice water content, both in the tropics and mid-latitudes. In particular the new scheme addresses the overriding weakness of the current diagnostic scheme, which produces almost no precipitation in the tropics. Instead the new scheme almost perfectly replicated both the pattern and quantity of tropical precipitation.

Tangent linear and adjoint versions of the new scheme have been constructed, and with some regularization to prevent instability, it is demonstrated that the scheme can successfully and robustly perform tangent linear integrations for a 12 hour window, and significantly improves the tangent linear approximation of the simplified linearized model to finite difference calculations using the full nonlinear forecast model.

With its physical link between cloud properties and the thermodynamic control variables of temperature and humidity, the new scheme provides the opportunity to develop a system which can assimilate both cloud and precipitation information. Moreau et al. (2003) have used the new cloud scheme in combination with the improved linearized convection scheme of Lopez and Moreau (2003). The approach was to use 1DVAR locally to obtain increments in total column water vapour, which are then inserted as 'pseudo observations' in the full 4D-VAR framework. This technique uses 1DVAR, which circumvents the stability problems that can arise in a pure 4D-Var framework. Chevallier et al. (2004) discuss the possibility of using the scheme to assimilate AIRS and Meteosat brightness temperatures in a 4DVAR framework, and this will be investigated further in a companion paper.

Acknowledgements

The authors would like to thank Anton Beljaars, Frederic Chevallier, Philippe Lopez, Martin Miller and Emmanuel Moreau for their valuable input and feedback concerning the new scheme and also this manuscript. The second author was supported by European Space Agency contract number 15740/01/NL/GS during part of this work.

References

Barker, H. W., 1996: A parameterization for computing grid-averaged solar fluxes for inhomogeneous marine boundary layer clouds. Part I: Methodology and homogeneous biases, *J. Atmos. Sci.*, **53**, 2289–2303.

Beheng, K. D., 1994: A parameterization of warm rain cloud microphysical processes, *Atmos. Res.*, **33**, 193–206.

Bony, S. and K. A. Emanuel, 2001: A parameterization of the cloudiness associated with cumulus convection; Evaluation using TOGA COARE data, *J. Atmos. Sci*, **58**, 3158–3183.

Bougeault, P., 1981: Modeling the trade-wind cumulus boundary-layer. Part I: Testing the ensemble cloud relations against numerical data, *J. Atmos. Sci.*, **38**, 2414–2428.

Brown, P. R. A. and H. A. Swann, 1997: Evaluation of key microphysical parameters in three dimensional cloud model simulations using aircraft and multiparameter radar data, *Q. J. R. Meteorol. Soc.*, **123**, 2245–2275.

Chevallier, F. and G. Kelly, 2002: Model clouds as seen from space: Comparison with geostationary imagery in the 11-micron window channel, *Mon. Wea. Rev.*, **130**, 712–722.

Chevallier, F., P. Lopez, A. M. Tompkins, M. Janisková, and E. Moreau, 2004: The capability of 4D-Var systems to assimilate cloud-affected satellite infrared radiances, *Q. J. R. Meteorol. Soc.*, submitted.

Courtier, P., J. N. Thepaut, and A. Hollingsworth, 1994: A strategy for operational implementation of 4D-Var, using an incremental approach, *Q. J. R. Meteorol. Soc.*, **120**, 1367–1387.

Ghan, S. J. and R. C. Easter, 1992: Computationally efficient approximations to stratiform cloud microphysics parameterization, *Mon. Wea. Rev.*, **120**, 1572–1582.

Golaz, J., V. E. Larson, and W. R. Cotton, 2002: A PDF-based parameterization for boundary layer clouds. Part I: Method and model description, *J. Atmos. Sci.*, **59**, 3540–3551.

Gregory, D., J. J. Morcrette, C. Jakob, A. C. M. Beljaars, and T. Stockdale, 2000: Revision of convection, radiation and cloud schemes in the ECMWF Integrated Forecasting System, *Q. J. R. Meteorol. Soc.*, **126**, 1685–1710.

Jakob, C., 1999: Cloud cover in the ECMWF reanalysis, *J. Climate*, **12**, 947–959.

Jakob, C., 2000: *The representation of cloud cover in atmospheric general circulation models*, PhD Thesis, ECMWF, Shinfield Park, Reading RG2 9AX, UK., pp190.

Jakob, C., 2002: Ice clouds in numerical weather prediction models: Progress, problems and prospects, in D. K. Lynch, K. Sassen, D. Starr, and G. Stephens, eds., *Cirrus*, Oxford University Press, pp. 327–345.

Jakob, C. and S. A. Klein, 2000: A parameterization of the effects of cloud and precipitation overlap for use in general-circulation models, *Q. J. R. Meteorol. Soc.*, **126**, 2525–2544.

Janisková, M., J.-F. Mahfouf, and J.-J. Morcrette, 2002a: Preliminary studies on the variational assimilation of cloud-radiation observations, *Q. J. R. Meteorol. Soc.*, **128**, 1505–1527.

Janisková, M., J.-F. Mahfouf, J.-J. Morcrette, and F. Chevallier, 2002b: Linearized radiation and cloud schemes in the ECMWF model: Development and evaluation, *Q. J. R. Meteorol. Soc.*, **128**, 1505–1527.

Janisková, M., J.-N. Thepaut, and J.-F. Geleyn, 1999: Simplified and regular physical parameterizations for incremental four-dimensional variational assimilation, *Mon. Wea. Rev.*, **127**, 26–45.

Kessler, E., 1969: *On the distribution and continuity of water substance in atmospheric circulation, Meteorological Monography, 10*, American Meteorological Society.

Khairoutdinov, M. and Y. Kogan, 2000: A new cloud physics parameterization in a large-eddy simulation model of marine stratocumulus, *Mon. Wea. Rev.*, **128**, 229–243.

Laroche, S., M. Tanguay, and Y. Delage, 2002: Linearization of a simplified planetary boundary layer parametrization, *Mon. Wea. Rev.*, **130**, 2074–2087.

Lenderink, G. and A. P. Siebesma, 2000: Combining the massflux approach with a statistical cloud scheme, in *Proc. 14th Symp. on Boundary Layers and Turbulence*, Amer. Meteor. Soc., Aspen, CO, USA, pp. 66–69.

LeTreut, H. and Z. X. Li, 1991: Sensitivity of an atmospheric general circulation model to prescribed SST changes: Feedback effects associated with the simulation of cloud optical properties, *Clim. Dyn.*, **5**, 175–187.

Lewellen, W. S. and S. Yoh, 1993: Binormal model of ensemble partial cloudiness, *J. Atmos. Sci.*, **50**, 1228–1237.

Lin, Y. L., R. D. Farley, and H. D. Orville, 1983: Bulk parameterization of the snow field in a cloud model, *J. Climate Appl. Meteor.*, **22**, 1065–1092.

Lohmann, U. and E. Roeckner, 1996: Design and performance of a new cloud microphysics scheme developed for the ECHAM general circulation model, *Clim. Dyn.*, **12**, 557–572.

Lopez, P., 2002: Implementation and validation of a new prognostic large-scale cloud and precipitation scheme for climate and data-assimilation purposes, *Q. J. R. Meteorol. Soc.*, **128**, 229–257.

Lopez, P. and E. Moreau, 2003: A convection scheme for data assimiliation purposes: Description and initial tests, Technical Report 411, European Centre for Medium-Range Weather Forecasts, Shinfield Park, Reading RG2 9AX, U.K.

Lord, S. J., 1982: Interaction of a cumulus cloud ensemble with the large-scale environment. Part III: Semi-prognostic test of the arakawa-schubert cumulus parameterization, *J. Atmos. Sci.*, **39**, 88–103.

Mahfouf, J.-F., 1999: Influence of physical processes on the tangent-linear approximation, *Tellus*, **51**, 147–166.

Mahfouf, J.-F., A. Beljaars, F. Chevallier, D. Gregory, C. Jakob, M. Janisková, J.-J. Morcrette, J. Teixeira, and P. Viterbo, 1999: The importance of the Earth radiation mission for numerical weather prediction, Technical Report 288, European Centre for Medium-Range Weather Forecasts, Shinfield Park, Reading RG2 9AX, U.K.

Mahfouf, J.-F. and F. Rabier, 2000: The ECMWF operational implementation of four-dimensional variational assimilation. I: Experimental results with improved physics, *Q. J. R. Meteorol. Soc.*, **126**, 1171–1190.

Morcrette, J. J., 2002: Assessment of the ECMWF model cloudiness and surface radiation fields at the ARM SGP site, *Mon. Wea. Rev.*, **130**, 257–277.

Moreau, E., P. Lopez, P. Bauer, A. M. Tompkins, M. Janisková, and F. Chevallier, 2003: Rainfall versus microwave brightness temperature assimilation: A comparison of 1D-Var results using TMI and SSM/I observations, *Q. J. R. Meteorol. Soc.*, **129**, submitted.

Rabier, F., E. Klinker, P. Courtier, and A. Hollingsworth, 1996: Sensitivity of forecast errors to initial conditions, *Q. J. R. Meteorol. Soc.*, **122**, 121–150.

Rabier, F., J.-N. Thepaut, and P. Courtier, 1998: Extended assimilation and forecast experiments with a four-dimensional variational assimilation system, *Q. J. R. Meteorol. Soc.*, **124**, 1861–1887.

Ricard, J. L. and J. F. Royer, 1993: A statistical cloud scheme for use in an AGCM, *Ann. Geophysicae*, **11**, 1095–1115.

Simmons, A. J., A. Untch, C. Jakob, P. Kållberg, and P. Undén, 1999: Stratospheric water vapour and tropical tropopause temperatures in ECMWF analyses and multi-year simulations, *Q. J. R. Meteorol. Soc.*, **125**, 353–386.

Slingo, J. M., 1987: The development and verification of a cloud prediction scheme for the ECMWF model, *Q. J. R. Meteorol. Soc.*, **113**, 899–927.

Smith, R. N. B., 1990: A scheme for predicting layer clouds and their water-content in a general-circulation model, *Q. J. R. Meteorol. Soc.*, **116**, 435–460.

Sommeria, G. and J. W. Deardorff, 1977: Subgrid-scale condensation in models of nonprecipitating clouds, *J.*

Atmos. Sci., **34**, 344–355.

Sundqvist, H., 1978: A parameterization scheme for non-convective condensation including prediction of cloud water content, *Q. J. R. Meteorol. Soc.*, **104**, 677–690.

Sundqvist, H., E. Berge, and J. E. Kristjansson, 1989: Condensation and cloud parameterization studies with a mesoscale numerical weather prediction model, *Mon. Wea. Rev.*, **117**, 1641–1657.

Teixeira, J., 2001: Cloud fraction and relative humidity in a prognostic cloud fraction scheme, *Mon. Wea. Rev.*, **126**, 1750–1753.

Tiedtke, M., 1989: A comprehensive mass flux scheme for cumulus parameterization in large-scale models., *Mon. Wea. Rev.*, **117**, 1779–1800.

Tiedtke, M., 1993: Representation of clouds in large-scale models, *Mon. Wea. Rev.*, **121**, 3040–3061.

Tompkins, A. M., 2002: A prognostic parameterization for the subgrid-scale variability of water vapor and clouds in large-scale models and its use to diagnose cloud cover, *J. Atmos. Sci.*, **59**, 1917–1942.

Walcek, C. J., 1994: Cloud cover and its relationship to relative-humidity during a springtime midlatitude cyclone, *Mon. Wea. Rev.*, **122**, 1021–1035.